

Inversion of walkaway VSP data in the presence of lateral velocity heterogeneity

Vladimir Grechka^{1,3}, Ilya Tsvankin¹, and Pedro Contreras²

¹*Center for Wave Phenomena, Department of Geophysics,
Colorado School of Mines, Golden, CO 80401*

²*PDVSA-INTEVEP, Apartado 76343, Caracas 1070A, Venezuela and*

³*presently at Marathon Oil*

(Dated: January 11, 2019)

Multi-azimuth walkaway vertical seismic profiling (VSP) is an established technique for the estimation of in situ slowness surfaces and inferring anisotropy parameters. Normally, this technique requires the assumption of lateral homogeneity, which makes the horizontal slowness components at depths of downhole receivers equal to those measured at the surface. Any violations of this assumption, such as lateral heterogeneity or nonzero dip of intermediate interfaces, lead to distortions in reconstructed slowness surfaces and, consequently, to errors in estimated anisotropic parameters.

Here, we relax the assumption of lateral homogeneity and discuss how to correct VSP data for *weak* lateral heterogeneity (LH). We describe a procedure of downward continuation of recorded traveltimes that accounts for the presence of both vertical inhomogeneity and weak lateral heterogeneity, which produces correct slowness surfaces at depths of downhole receivers. Once the slowness surfaces are found and a desired type of anisotropic model to be inverted is selected, the corresponding anisotropic parameters, providing the best fit to the estimated slownesses, can be obtained. We invert the slowness surfaces of P -waves for parameters of the simplest anisotropic model describing dipping fractures – transversely isotropic medium with a tilted symmetry axis. Five parameters of this model – the P -wave velocity V_0 in the direction of the symmetry axis, Thomsen’s anisotropic coefficients ϵ and δ , the

tilt ν , and the azimuth β of the symmetry axis can be estimated in a stable manner when maximum source offset is greater than half of receiver depth.

Keywords: walkaway VSP, lateral velocity heterogeneity, anisotropic parameter estimation

PACS numbers: 91.30.Cd 91.60.Ba 91.30.pc 91.30.Ab

I. INTRODUCTION

Obtaining anisotropic velocity fields is one of the main challenges in extending seismic processing to anisotropic media. Although analysis of P -wave surface reflection data allows one to estimate subsets of anisotropic parameters sufficient for time processing, the vertical velocity usually remains undetermined in such important for exploration anisotropic models as transversely isotropic with a vertical symmetry axis (VTI) [1] and orthorhombic (ORT) [5, 7]. Lack of information about vertical velocity leads to distortions in a vertical scale of depth-migrated seismic sections, routinely observed in areas with non-negligible anisotropy. One possible way to obtain the true vertical velocity and, therefore, correct depth images in VTI and ORT media [1, 13] is to explicitly measure velocity using check shots or near-offset vertical seismic profiling (VSP) data.

Traveltimes of direct P -arrivals recorded in multi-azimuth walkaway VSP geometry provide information not only about true vertical velocity but also about some portion of the slowness surface, which can be used to reconstruct in situ anisotropic parameters. The principal scheme of obtaining the slowness surface [3] is shown in Figure 1. The horizontal p_i ($i = 1, 2$) and vertical q components of the slowness vector are, by definition, the components of traveltime gradient, i.e.,

$$p_i = \frac{\partial t}{\partial x_i} \quad \text{and} \quad q = \frac{\partial t}{\partial z}. \quad (1)$$

Therefore, having measured traveltimes between several surface sources located along coordinate axes x_1 and x_2 of a selected coordinate frame and downhole receiver at the depth z , we can calculate the horizontal slowness components p_i (Figure 1a). Using traveltimes recorded for a given source and several downhole receivers, we can find the vertical slowness component q (Figure 1b). The problem, however, is that the horizontal slowness components are measured *at the surface* while the vertical component is obtained *at the receiver depth*.

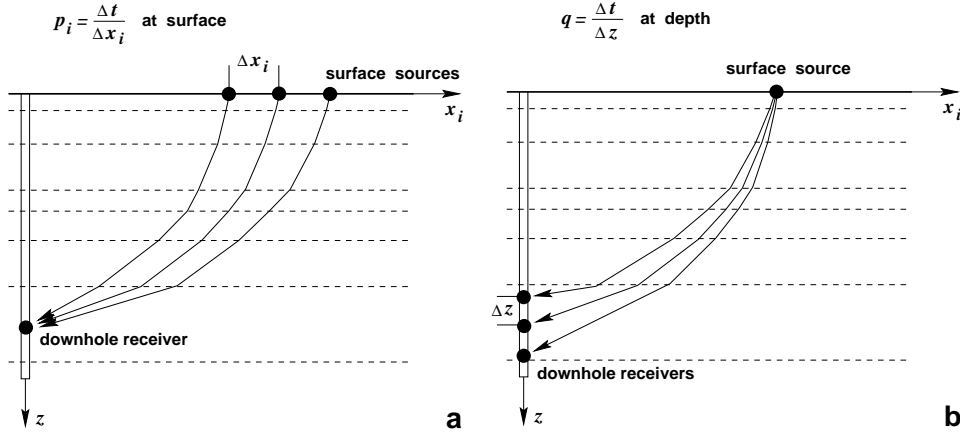


FIG. 1: Principal scheme of calculating (a) the horizontal components p_i ($i = 1, 2$) of the slowness vector and (b) its vertical component q [3].

If medium above receiver is laterally homogeneous, the measured horizontal slowness components p_i are preserved along downward propagating rays due to Snell's law and become equal to those at receiver depth, thus, giving local value of slowness $q(p_1, p_2)$ at the depth z . The assumption of lateral homogeneity is conventionally made in the papers on estimation of anisotropic parameters from VSP data [3, 8, 9].

On the other hand, it is known that if this assumption is violated due to the presence of lateral heterogeneity or nonzero dip of intermediate interfaces, erroneous values of q as function of p_1 and p_2 are obtained [3]. For example, Sayers in 1997 [14] found that dip of an intermediate interface of only 5° significantly distorts $q(p_1, p_2)$ values.

Here, we show that information about LH contained in traveltimes recorded in VSP geometry can be, under certain circumstances, extracted and the influence of LH on traveltimes can be removed. The assumptions we make are the following:

1. The medium is vertically homogeneous at each interval between downhole receivers.
2. Anisotropy is factorized with respect to lateral coordinates, i.e., anisotropy coefficients are constant at each interval while velocity itself may vary laterally.
3. Lateral heterogeneity is weak.

The first two assumptions allow us to separate the influence of LH on traveltimes from those of vertical inhomogeneity and anisotropy; the third assumption makes it possible to

linearize traveltimes with respect to LH and derive explicit equations expressing the contribution of LH. Based on these equations, we develop a procedure to propagate the recorded traveltimes downward and compute slowness surfaces $q(p_1, p_2)$ at receiver depths. We present numerical examples illustrating improvements in accuracy of reconstructed slowness surfaces compared to those obtained using the conventional approach.

To invert anisotropy parameters from the best fit of computed and extracted slowness surfaces, a certain anisotropic model has to be chosen. Usually, only P -wave slownesses are obtained and inversion is performed for models with horizontal symmetry plane – VTI [3] or orthorhombic [8]. Since this sort of inversion does not require anisotropic medium to possess a horizontal symmetry plane, we assume the model to be transversely isotropic with a *tilted* symmetry axis (TTI model) and estimate its five parameters: the P -wave velocity V_0 in the direction of the symmetry axis, generic [15] anisotropic coefficients ϵ and δ , and the tilt ν and azimuth β of the symmetry axis.

II. AMBIGUITY BETWEEN ANISOTROPY AND LATERAL HETEROGENEITY

We begin our discussion with an example illustrating that lateral heterogeneity, even perceived as insignificant, does present a problem for conventional approach of estimating slowness surfaces and lead to erroneous conclusions about anisotropy of the subsurface. Figure 2a shows the contours of P -wave traveltime surface $t(x_1, x_2)$ recorded by the receiver at depth $z = 1$ km located in vertical borehole with coordinates $[x_1, x_2] = [0, 0]$ km. The traveltimes were computed numerically using the technique described by Grechka and McMechan [4] in a purely isotropic model with linear lateral velocity variation $V_0(x_1, x_2) = 2.0 - 0.1(x_1 + x_2)$ [in km/s]. Velocity heterogeneity in this model can be characterized by the absolute value of lateral velocity gradient $h = 0.1 \text{ s}^{-1}$ or by the velocity variance which is equal to only 2.7% for the offsets x_1 and x_2 shown in Figure 2a. Nevertheless, lateral heterogeneity clearly manifests itself by shifting the traveltime minimum (marked with the plus in Figure 2a) away from the zero offset. In principle, this shift can be attributed to any combination of the following three factors: 1) lateral heterogeneity in the subsurface; 2) anisotropy without horizontal symmetry plane; and 3) uncertainty in the lateral receiver position. We assume the receiver location to be known exactly and analyze the influences of the first two factors.

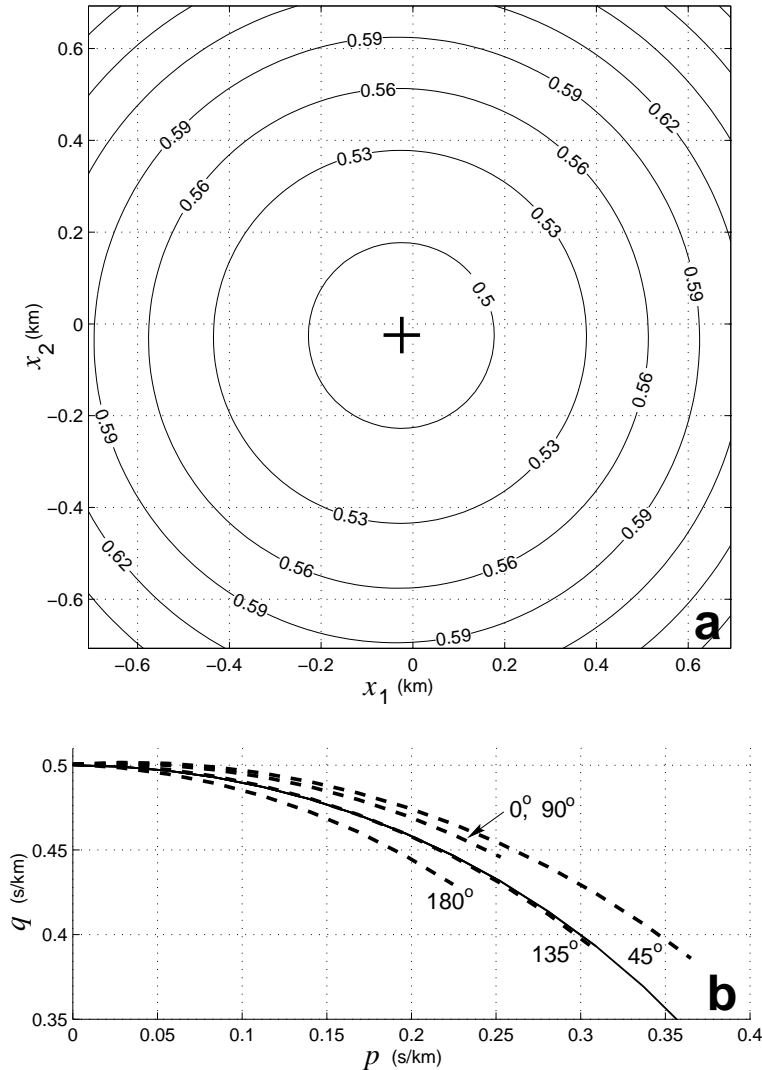


FIG. 2: (a) Contours (in s) of traveltime surface $t(x_1, x_2)$ recorded at depth $z = 1$ km in isotropic model with laterally varying velocity $V_0(x_1, x_2) = 2.0 - 0.1(x_1 + x_2)$ [km/s]. The sign “+” indicates the position of traveltime minimum. (b) Cross-sections of the slowness surface $q(p_1, p_2)$, where $p_1 = p \cos \alpha$ and $p_2 = p \sin \alpha$, at azimuths $\alpha = 0^\circ, 45^\circ, 90^\circ, 135^\circ$, and 180° (with respect to axis x_1) reconstructed under the assumption of lateral homogeneity (dashed) and cross-section of the correct isotropic slowness surface (solid).

Conventionally, one would assume lateral homogeneity and explain the shift of the traveltime minimum from the zero offset by anisotropy. Following this approach, we calculated the derivatives $p_i = \partial t / \partial x_i$ of the traveltime shown in Figure 2 and estimated $q = \partial t / \partial z$ using traveltimes computed for the array of receivers at depths $z = [0.98, 0.99, 1.00, 1.01, 1.02]$ km.

Then, we reconstructed the slowness surface $q(p_1, p_2)$. Its cross-sections along several azimuthal directions, shown in Figure 2b, clearly indicate the presence of apparent *azimuthal anisotropy*. Note that the deviation from the correct slowness surface (solid line in Figure 2b) is the greatest in the direction of lateral velocity gradient (azimuth $\alpha = 45^\circ$) and smallest in the orthogonal direction at azimuth $\alpha = 135^\circ$. This observation is analogous to the result of Sayers (1997) [14], who studied the influence of dipping interfaces in the overburden on recovering the slownesses in VTI media and concluded that the influence of dip is negligible for acquisition in the strike direction. The next question, which might be asked, is whether one can find an anisotropic model that explains the cross-sections of $q(p_1, p_2)$ surface in Figure 2b. This model has to be azimuthally anisotropic as obvious from Figure 2b. Also, it is not supposed to have a horizontal symmetry plane because otherwise it would be impossible to explain the shift of the traveltime minimum seen in Figure 2a. The simplest anisotropic model satisfying both requirements is TTI – transversely isotropic with a tilted symmetry axis. The P -wave slowness surface in this model, being insensitive to the shear-wave velocity (Grechka and Tsvankin, 1998) [6], is determined by five quantities: the P -wave velocity V_0 in the direction of the symmetry axis, Thomsen’s (1986) coefficients ϵ and δ , the tilt ν , and the azimuth β of the symmetry axis. We invert the vector $\chi \equiv [V_0, \epsilon, \delta, \nu, \beta]$ containing those five quantities by minimizing the least-squares objective function

$$\mathcal{F}(\chi) = \left[\frac{\sum_{j=1}^N \left(q(p_1^{(j)}, p_2^{(j)}) - \tilde{q}(p_1^{(j)}, p_2^{(j)}, \chi) \right)^2}{N - 1} \right]^{\frac{1}{2}} \quad (2)$$

that expresses the standard deviation of N computed vertical slownesses \tilde{q} from the vertical slownesses q measured from VSP traveltimes. The slownesses $\tilde{q}(p_1^{(j)}, p_2^{(j)}, \chi)$ are calculated from the Christoffel equation [10]. The minimization of the objective function \mathcal{F} is carried out using the simplex method (Press et al., 1987) [12].

Table 1 shows parameters of the obtained TTI model along with parameters of the true isotropic model. Although the values of velocity V_0 in the direction of the symmetry axis and anisotropy coefficients ϵ and δ are seriously distorted, there is some logic in the obtained azimuth $\beta = 45^\circ$. Note, this azimuth, picked by the inversion algorithm, is equal to the azimuth of lateral velocity gradient and corresponds to the direction of the vertical symmetry plane which exists in both homogeneous TTI and LH isotropic models. The parameters of inverted TTI model presented in Table 1 produce the value of the objective function

Model 1	V_0 (km/s)	h (s ⁻¹)	ϵ	δ	ν	β
Correct (LH isotropic)	2.00	0.1	0.0	0.0	–	–
Inverted (homogeneous TTI)	1.52	0.0	0.29	0.11	14.9	45.0

Table 1. Parameters of correct LH isotropic model and inverted homogeneous TTI model. The tilt ν and the azimuth β (with respect to direction x_1 in Figure 2a) of the symmetry axis in inverted TTI model are given in degrees.

$\mathcal{F} = 0.0013$, which corresponds to the standard deviation of \tilde{q} from q [see equation (2)] of only 0.26% relative to the measured $q|_{p=0} = 0.5$ s/km at zero horizontal slowness (Figure 2b). Thus, the homogeneous TTI model with parameters from Table 1 accurately fits the slowness surface obtained from VSP data in the isotropic LH model.

III. CORRECTION FOR LATERAL HETEROGENEITY IN A SINGLE LAYER

In this section, we derive an explicit correction for lateral heterogeneity of traveltimes recorded in VSP experiment. We consider a single, vertically homogeneous layer (Figure 3) where the group velocity g can be represented in the *factorized* form:

$$g(\theta, \alpha, y_1, y_2) = g^{\text{hom}}(\theta, \alpha) f(y_1, y_2), \quad (3)$$

where $g^{\text{hom}}(\theta, \alpha)$ is the group velocity in a homogeneous anisotropic background medium. Since the ray \mathbf{r}^{hom} between the source at $[x_1, x_2, 0]$ and the receiver at $[0, 0, z]$ in the background medium is a straight line, g^{hom} is a function of two directional angles – the polar angle θ and the azimuth α (Figure 3). The factor $f(y_1, y_2)$, which depends on horizontal coordinates y_1 and y_2 along a ray, represents lateral variation of the group velocity. We assume that lateral heterogeneity not only factorized [for this reason, g is the product of g^{hom} and f in equation(3)] but also *weak*, which means that

$$f(y_1, y_2) \approx 1. \quad (4)$$

It is convenient to express the factor $f(y_1, y_2)$ as a polynomial of finite power M

$$f(y_1, y_2) \equiv 1 + \Psi(y_1, y_2) = 1 + \sum_{m=1}^M \sum_{\ell=0}^m \psi_{\ell, m-\ell} y_1^\ell y_2^{m-\ell} \quad (5)$$

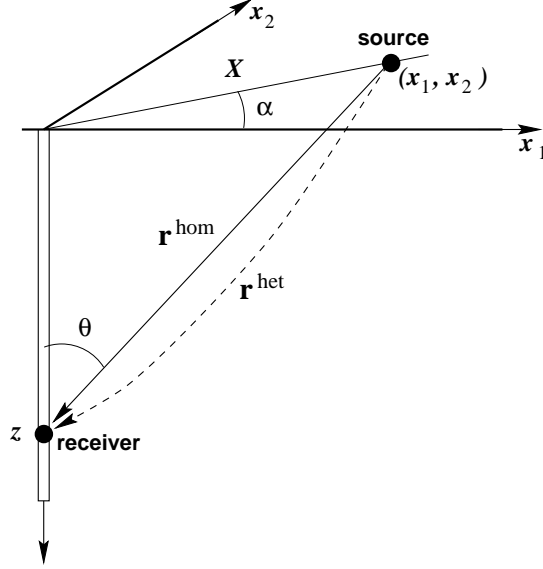


FIG. 3: In deriving linearized correction for weak lateral heterogeneity, traveltimes can be integrated along the straight ray \mathbf{r}^{hom} (solid) in a homogeneous background model. The actual bending ray \mathbf{r}^{het} (dashed) does not need to be considered.

with some coefficients $\psi_{\ell, m-\ell}$. Equation (4) implies the inequality

$$|\Psi(y_1, y_2)| \ll 1. \quad (6)$$

We are interested in deriving the first-order correction of traveltimes due to the presence of lateral heterogeneity. Therefore, we linearize the traveltimes with respect to LH and ignore all terms containing quadratic and higher-order combinations of coefficients $\psi_{\ell, m-\ell}$. In the linear approximation, the traveltimes t^{LH} between the source and receiver in Figure 3 can be calculated as an integral along the ray \mathbf{r}^{hom} in the background medium (e.g., Backus and Gilbert, 1969) [2]:

$$t^{\text{LH}}(x_1, x_2, z) = \frac{\sqrt{X^2 + z^2}}{X} \int_0^X \frac{d\xi}{g(\theta, \alpha, y_1(\xi), y_2(\xi))}, \quad (7)$$

where

$$x_1 = X \cos \alpha \quad \text{and} \quad x_2 = X \sin \alpha; \quad (8)$$

X is the offset, ξ is the lateral coordinate along the straight ray \mathbf{r}^{hom} . The coordinates y_1 and y_2 relate to ξ as

$$y_1 = \xi \cos \alpha \quad \text{and} \quad y_2 = \xi \sin \alpha. \quad (9)$$

Evaluating integral (7) in the linear approximation with respect to $\psi_{\ell,m-\ell}$ yields

$$t^{\text{LH}}(x_1, x_2, z) = t^{\text{hom}}(x_1, x_2, z) \mathcal{H}(x_1, x_2), \quad (10)$$

where

$$t^{\text{hom}}(x_1, x_2, z) = \frac{\sqrt{X^2 + z^2}}{g^{\text{hom}}(\theta, \alpha)} \quad (11)$$

is the travelttime in the background medium, and the factor

$$\mathcal{H}(x_1, x_2) \equiv 1 + H(x_1, x_2) = 1 - \sum_{m=1}^M \frac{1}{m+1} \sum_{\ell=0}^m \psi_{\ell,m-\ell} x_1^\ell x_2^{m-\ell} \quad (12)$$

will be called the heterogeneity factor. Comparing equations (5) and (12), we conclude that, according to inequality (6), the magnitude of polynomial $H(x_1, x_2)$ has to be small, i.e.,

$$|H(x_1, x_2)| \ll 1. \quad (13)$$

A. Accounting for lateral heterogeneity

Equation (10), the main result of previous section, holds in arbitrarily anisotropic, factorized, weakly LH media. Here, we use it to infer the velocity function specified by coefficients $\psi_{\ell,m-\ell}$ from measured travelttime t^{LH} and its derivatives

$$p_i^{\text{LH}} \equiv \frac{\partial t^{\text{LH}}}{\partial x_i} \quad \text{and} \quad q^{\text{LH}} \equiv \frac{\partial t^{\text{LH}}}{\partial z}, \quad (i = 1, 2). \quad (14)$$

Substituting equation (10) into equations (14) yields

$$p_i^{\text{LH}} = p_i^{\text{hom}} \mathcal{H} + t^{\text{hom}} \frac{\partial \mathcal{H}}{\partial x_i} \quad \text{and} \quad q^{\text{LH}} = q^{\text{hom}} \mathcal{H}, \quad (15)$$

where, by definition,

$$p_i^{\text{hom}} \equiv \frac{\partial t^{\text{hom}}}{\partial x_i} \quad \text{and} \quad q^{\text{hom}} \equiv \frac{\partial t^{\text{hom}}}{\partial z}. \quad (16)$$

Travelttime t^{hom} and components of the slowness vector in homogeneous anisotropic media relate as

$$p_1^{\text{hom}} x_1 + p_2^{\text{hom}} x_2 + q^{\text{hom}} z = t^{\text{hom}}. \quad (17)$$

This equation follows from the relation between the slowness and the group velocity vectors (e.g., Musgrave, 1970) [10]

$$p_1^{\text{hom}} g_1^{\text{hom}} + p_2^{\text{hom}} g_2^{\text{hom}} + q^{\text{hom}} g_3^{\text{hom}} = 1. \quad (18)$$

Using the measured quantities p_i^{LH} , q^{LH} , and t^{LH} , we construct the *known* quantity

$$\mathcal{R} = \frac{1}{t^{\text{LH}}} (p_1^{\text{LH}} x_1 + p_2^{\text{LH}} x_2 + q^{\text{LH}} z) - 1. \quad (19)$$

Taking into account equations (10), (12), (15) and (17), equation (19) can be reduced to

$$\mathcal{R} (1 + H) = \frac{\partial H}{\partial x_1} x_1 + \frac{\partial H}{\partial x_2} x_2. \quad (20)$$

This equation allows us to find H or the coefficients $\psi_{\ell, m-\ell}$ [see equation (12)] defining velocity heterogeneity. We express \mathcal{R} as a polynomial

$$\mathcal{R}(x_1, x_2) = \sum_{m=1}^M \sum_{\ell=0}^m R_{\ell, m-\ell} x_1^\ell x_2^{m-\ell} \quad (21)$$

and note that $\mathcal{R}(x_1, x_2)$ does not have a constant (i.e., independent on x_i) term because there is no such a term in the right-hand side of equation (20). Also, due to inequality (13), the magnitude of polynomial \mathcal{R} is small. Substituting equations (12) and (21) into equation (20) and solving this equation in the linear approximation for the coefficients $\psi_{\ell, m-\ell}$ yields the set of explicit relations

$$\psi_{\ell, m-\ell} = -\frac{m+1}{m} R_{\ell, m-\ell}. \quad (22)$$

Thus, we have obtained the following algorithm to remove the influence of LH on VSP data:

- construct the function \mathcal{R} given by equation (19) from the measured quantities p_i^{LH} , q^{LH} , and t^{LH} ;
- represent $\mathcal{R}(x_1, x_2)$ as the polynomial (21) and, using equation (22), compute the coefficients ψ of the function f [equation (5)] describing lateral velocity heterogeneity;
- build the heterogeneity factor \mathcal{H} [equation (12)] and reconstruct the slowness components p_i^{hom} and q^{hom} in the homogeneous background medium using equations (10) and (15).

IV. NUMERICAL EXAMPLES

Here, we present several numerical examples to test the technique developed in the previous section. We begin with the isotropic LH model from Table 1. Our algorithm accurately reconstructed lateral velocity gradient and produced the slowness surface which

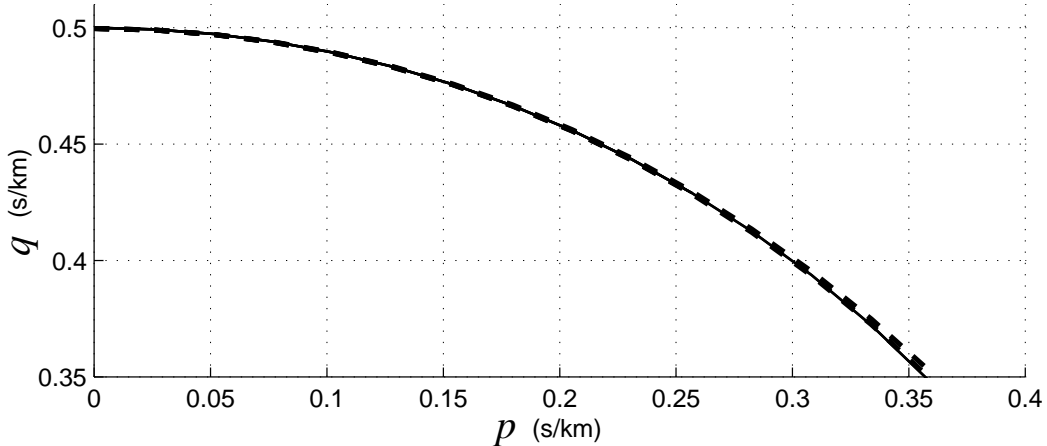


FIG. 4: Cross-sections of the slowness surface $q(p \cos \alpha, p \sin \alpha)$ at azimuths $\alpha = 0^\circ, 45^\circ, 90^\circ, 135^\circ,$ and 180° reconstructed after accounting for lateral heterogeneity (overlapping dashed lines) and cross-section of the correct isotropic slowness surface (solid line). Parameters of the correct model are given in Table 1.

cross-sections are shown in Figure 4 (compare it with Figure 2b). The cross-sections at different azimuths overlap each other and the correct isotropic cross-section. There is small deviation at large values of p where LH influences traveltimes stronger. We inverted the reconstructed slowness surface and obtained the following set of parameters of TTI medium: $V_0 = 1.99$ km/s, $\epsilon = 0$, $\delta = 0.01$, $\nu = 41.7^\circ$, and $\beta = 45.0^\circ$ (compare these parameters with the correct parameters in Table 1). Interestingly, that the inversion algorithm again picked up the azimuth $\beta = 45^\circ$ of the vertical symmetry plane of the model.

An alternative approach to account for lateral velocity variations is to replace the horizontal slowness components with the P -wave polarization directions [11]. The authors of paper [11], published later, derived the P -wave slowness on polarization dependence, established its governing parameters, and estimated those parameters from a P -wave VSP data set acquired in the deep-water Gulf of Mexico (see Figure 1 in Grechka and Mateeva [11] and references therein).

In the second test, we estimate parameters of LH TTI model in Table 2. This time, the shift of traveltime minimum (marked with the plus in Figure 5a) from the coordinate origin is due to the influence of both anisotropy without horizontal symmetry plane and lateral heterogeneity. The technique described in the previous section has been able to separate

Model 2	V_0 (km/s)	ϵ	δ	ν	β
Correct	$2.00 (1 + 0.100x_1 + 0.030x_2 + 0.010x_1^2)$	0.250	0.150	30.0	-90.0
Inverted	$1.98 (1 + 0.100x_1 + 0.029x_2 + 0.003x_1^2)$	0.252	0.149	29.6	-90.0

Table 2. Parameters of correct and inverted LH TTI models. The tilt ν and the azimuth β of the symmetry axis are given in degrees.

these two influences and resulted in the cross-sections of the slowness surface shown in Figure 5b with dashed lines. Their small deviations from the correct cross-sections (solid lines in Figure 5b) can be explained by the approximations made with respect to lateral heterogeneity. The inverted anisotropic parameters are given in Table 2. Although there are some errors in the estimated parameters, the algorithm has performed fairly well.

In our last test in this section, we examine what happens if the assumption of factorized anisotropy is violated, and both the velocity V_0 and anisotropic coefficients change laterally. The model parameters are shown in Table 3. Three quantities – V_0 , δ , and ν – vary. While variation of δ is relatively small (it changes from 0.126 to 0.174 with the mean value equal to 0.15), the variation of the tilt ν is more pronounced. The tilt varies from $\nu = 17.1^\circ$ to $\nu = 40.1^\circ$, the mean tilt is 28.6° . Again, we apply the same technique to estimate the influence of LH, remove it, and infer parameters of TTI medium assuming that *anisotropy is factorized*. The inversion results are presented in Table 3. We did not reconstruct lateral variations of anisotropic coefficients, instead, we obtained their single values which happened to be close to the corresponding correct mean values. This suggests that the assumption of factorized anisotropy is not that important, and obtaining some reasonable estimates of anisotropic parameters, close to their mean values, can be expected.

V. AMBIGUITY BETWEEN VERTICAL HETEROGENEITY VI AND LATERAL HETEROGENEITY LH

Since vertical inhomogeneity (VI) is usually stronger than lateral heterogeneity LH, it is important to develop a technique that would allow one to account for LH *in the presence of* VI. First, we show that the required data should contain traveltimes recorded at a sufficiently dense set of downhole receivers, otherwise it is impossible to separate the influences of LH

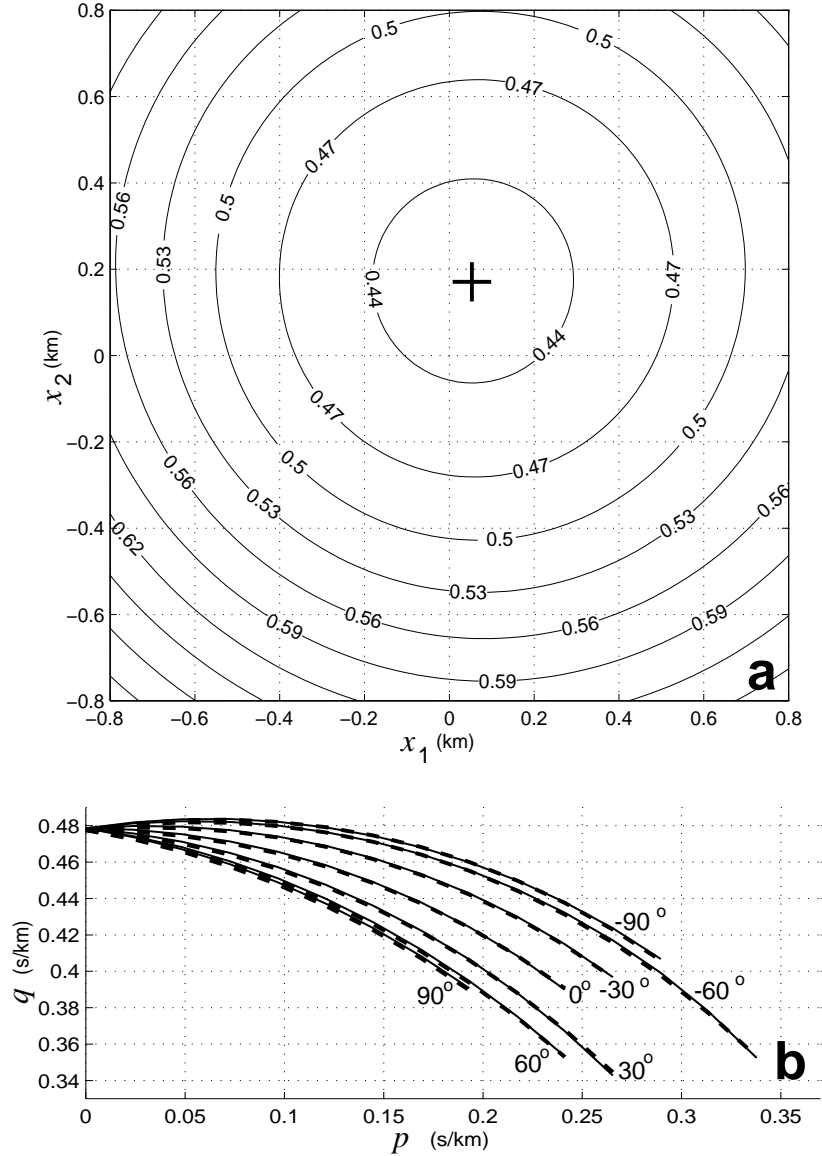


FIG. 5: (a) Contours (in s) of traveltime $t^{\text{LH}}(x_1, x_2)$ recorded at depth $z = 0.94$ km. The “+” sign indicates the position of traveltime minimum. (b) Cross-sections of the slowness surface $q^{\text{hom}}(p_1^{\text{hom}}, p_2^{\text{hom}})$, where $p_1^{\text{hom}} = p \cos \alpha$ and $p_2^{\text{hom}} = p \sin \alpha$, at azimuths $\alpha = -90^\circ, -60^\circ, -30^\circ, 0^\circ, 30^\circ, 60^\circ$, and 90° reconstructed after accounting for lateral heterogeneity (dashed) and cross-sections of the correct TTI slowness surface (solid).

and VI on VSP data even though there are measurements of the vertical velocity along a borehole.

Suppose we record traveltimes in the VSP geometry (Figure 6), where surface sources have a large aperture whereas downhole receivers cover only a relatively small range of

Model 3	ϵ	δ	ν	β
Correct	0.250	variable	variable	-90.0
Inverted	0.251	0.158	30.1	-90.2

Table 3. Parameters of correct and inverted LH TTI models. The lateral variation of velocity V_0 is the same as that in Model 2 (Table 2). The anisotropy coefficient δ changes in the direction x_2 as $\delta = 0.15(1.0 + 0.2x_2)$. The lateral variation of the tilt ν is $\nu = \arcsin[0.5 + 0.125(x_1 - x_2)]$.

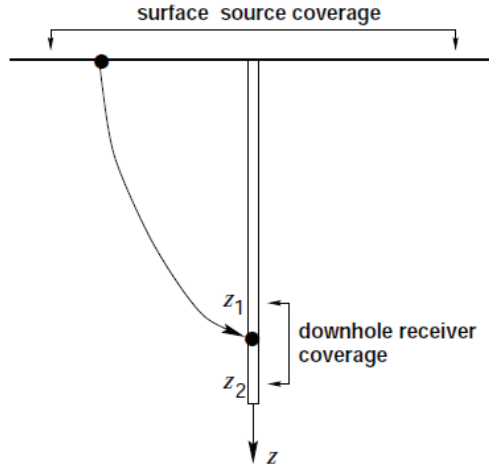


FIG. 6: VSP data with only partial coverage of downhole receivers do not allow one to distinguish between lateral and vertical heterogeneity.

depths $z_1 \leq z \leq z_2$. We assume that the depth coverage is just sufficient to calculate the derivative $\partial t/\partial z$ [i.e., $(z_2 - z_1)/z_2 \ll 1$] and find the vertical slowness q at depth z . As a test, we examine what can be reconstructed from the traveltimes t^{VI} and the vertical slowness q^{VI} in elliptically anisotropic VTI model with horizontal velocity changing linearly with depth (Table 4). Figure 7a shows traveltimes t^{VI} (dotted line) calculated using an exact equation in elliptically anisotropic VI medium with parameters from Table 4. The traveltimes t^{VI} corresponds to the receiver depth $z = 1$ km, where Thomsen's anisotropic coefficients ϵ and δ reach 0.28 indicating significant anisotropy. Despite that, traveltimes t^{VI} virtually coincides with traveltimes t^{LH} (solid line) computed numerically in LH medium with non-elliptical anisotropy (parameters of this medium are given in Table 4; the function $V_0(x)$ is shown in Figure 7b). The maximum difference between traveltimes t^{VI} and t^{LH} is only 0.3%, illustrating a high accuracy of the approximations made and also showing that both

Model 4	Vertical velocity	ϵ	δ
Correct (VI)	$V_0 = \text{const}$	$kz + \frac{(kz)^2}{2}$	$kz + \frac{(kz)^2}{2}$
Inverted (LH)	$V_0 \left(1 + \frac{3k}{4z} x^2 - \frac{5k}{8z^3} x^4 \right)$	$\frac{kz}{8}$	$\frac{kz}{4}$

Table 4. Parameters of correct and inverted VTI models. The correct vertically inhomogeneous model is elliptically anisotropic. It has constant vertical velocity V_0 and depth-varying anisotropic coefficients $\epsilon = \delta$. The inverted model is laterally heterogeneous. Its vertical velocity changes laterally and anisotropy is not elliptical ($\epsilon \neq \delta$).

traveltimes are indistinguishable.

The results of reconstruction of the slownesses are presented in Figure 7c. While the solid line represents elliptical dependence that has been estimated assuming vertically inhomogeneous model, the dashed line (close to the circular dotted line) shows quite different function obtained under the assumption that the model is laterally heterogeneous. Since both models fit the traveltimes and the vertical slowness measured at single depth z , it is impossible to infer the type of heterogeneity – vertical versus lateral – from the data.

A. Correcting for LH in the presence of VI

To distinguish between lateral and vertical heterogeneity, it is necessary to acquire VSP data with such a dense sampling along a borehole that the medium between adjacent receivers can be considered vertically homogeneous. Then, the problem reduces to the sequence of parameter estimation steps for each interval between adjacent receivers (or groups of receivers; the groups are needed to estimate the vertical slowness component) followed by downward propagation of traveltimes within the intervals.

The algorithm is illustrated in Figure 8. Let us suppose that the data contain two sets of traveltimes $t^{\text{LH}}(n)$ and vertical slowness components $q^{\text{LH},(n)}$ ($n = 1, 2$) recorded between the sources $S^{(1)}$ at the surface $z^{(0)}$ and receivers $R^{(n)}$ at depths $z^{(n)}$. The in-

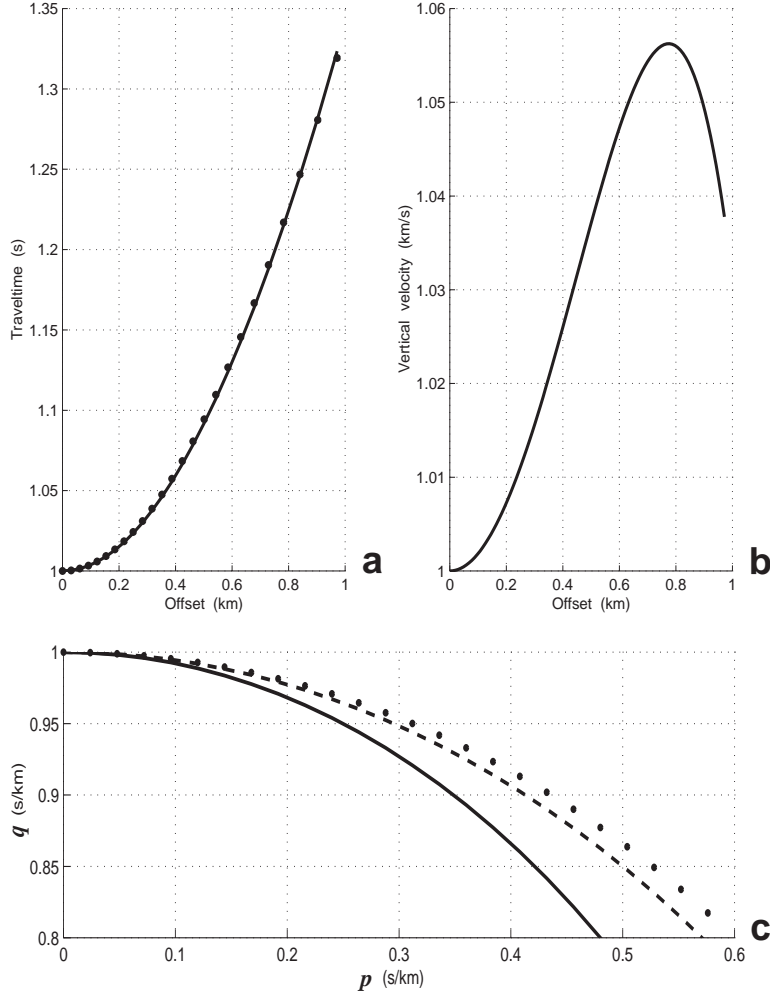


FIG. 7: (a) Traveltimes in VTI models from Table 4: t^{VI} (dotted) calculated under the assumption of VI using exact expression, and t^{LH} (solid) computed numerically in the LH model. (b) Lateral variation of the vertical velocity $V_0(x)$ given in Table 4. (c) Slowness curves: in VI model (solid) and in LH model (dashed). The dotted line indicates a circle. Model parameters: $V_0 = 1$ km/s, $k = 0.25$ km $^{-1}$. The depth of downhole receiver $z = 1$ km.

index n denotes traveltimes measured by receiver $R^{(n)}$; n in the superscript refers to the interval quantities. We assume that the distances $z^{(n)} - z^{(n-1)}$ are sufficiently small so that the medium at each interval can be considered vertically homogeneous. We can apply the above described method to the measured traveltimes $t^{\text{LH}}(1) = t^{\text{LH},(1)}$ and vertical slowness components $q^{\text{LH},(1)}$ to estimate velocity heterogeneity $f^{(1)}$ [equation (3)], the slowness vectors $\mathbf{p}^{\text{hom},(1)} = [p_1^{\text{hom},(1)}, p_2^{\text{hom},(1)}, q^{\text{hom},(1)}]$, and vector of anisotropic parameters $\chi^{(1)} = [V_0^{(1)}, \epsilon^{(1)}, \delta^{(1)}, \nu^{(1)}, \beta^{(1)}]$ in the first interval between the levels $z^{(0)}$ and $z^{(1)}$.

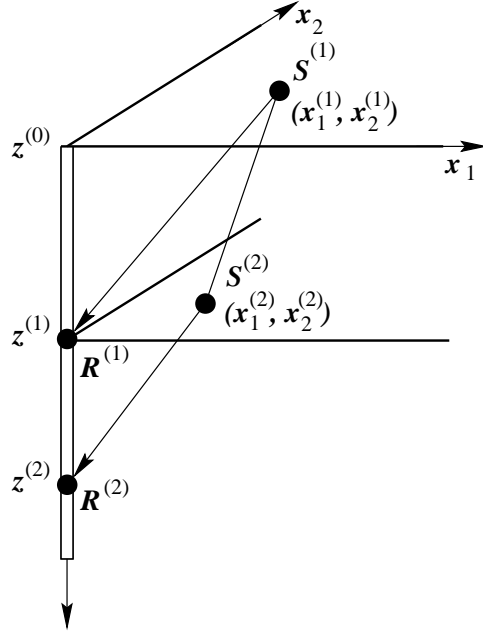


FIG. 8: Accounting for LH in the presence of VI can be done in two steps. First, we remove LH and estimate anisotropic parameters in the interval $[z^{(0)}, z^{(1)}]$ above receiver $R^{(1)}$ applying the technique developed for a single layer. Second, we use obtained parameters to map the traveltme measured between the source $S^{(1)}$ and receiver $R^{(2)}$ onto the depth level $z^{(1)}$. Then, we repeat the first step to find parameters in the interval $[z^{(1)}, z^{(2)}]$ between receivers $R^{(1)}$ and $R^{(2)}$.

Next, we take the measured traveltimes $t^{\text{LH}}(2)$ between the sources $S^{(1)}$ located at $[x_1^{(1)}, x_2^{(1)}, z^{(0)}]$ and the receiver $R^{(2)}$ at $[0, 0, z^{(2)}]$ (Figure 8) and find the horizontal slowness components $p_i^{\text{LH},(1)} = \partial t^{\text{LH}}(2) / \partial x_i$ at level $z^{(0)}$. Using the assumption of factorized anisotropy, the horizontal slowness components in the background medium can be computed as

$$p_i^{\text{hom},(1)} = p_i^{\text{LH},(1)} f^{(1)}, \quad (i = 1, 2). \quad (23)$$

Then, the value of $q^{\text{hom},(1)}$ is obtained from the already known vectors $\mathbf{p}^{\text{hom},(1)}$. This allows us to shoot rays from the sources $S^{(1)}$ downward and find lateral coordinates of the points $S^{(2)}$ at the level $z^{(1)}$:

$$x_i^{(2)} = x_i^{(1)} - \frac{g_i^{\text{hom},(1)}}{g_3^{\text{hom},(1)}} (z^{(1)} - z^{(0)}) = x_i^{(1)} + q_i^{\text{hom},(1)} (z^{(1)} - z^{(0)}), \quad (24)$$

where $q_i^{\text{hom},(1)} \equiv \partial q^{\text{hom},(1)} / \partial p_i^{\text{hom},(1)}$, and the relation $q_i^{\text{hom},(1)} = -g_i^{\text{hom},(1)} / g_3^{\text{hom},(1)}$ is obtained by differentiating equation (18).

The traveltimes $t^{\text{LH},(1)}$ in the depth interval $[z^{(0)}, z^{(1)}]$ between the points $S^{(1)}$ at $[x_1^{(1)}, x_2^{(1)}, z^{(0)}]$ and $S^{(2)}$ at $[x_1^{(2)}, x_2^{(2)}, z^{(1)}]$ can be calculated based on equation (7) under the assumption of weak lateral heterogeneity:

$$t^{\text{LH},(1)} = \sqrt{1 + \frac{\Delta z^2}{\Delta X^2}} \int_0^{\Delta X} \frac{d\xi}{g^{\text{hom},(1)} f^{(1)}(y_1(\xi), y_2(\xi))}, \quad (25)$$

where

$$\Delta X = \left[\left(x_1^{(2)} - x_1^{(1)} \right)^2 + \left(x_2^{(2)} - x_2^{(1)} \right)^2 \right]^{\frac{1}{2}},$$

$$\Delta z = z^{(1)} - z^{(0)},$$

$$y_1 = x_1^{(1)} + \xi \cos \alpha,$$

$$y_2 = x_2^{(1)} + \xi \sin \alpha,$$

and

$$\tan \alpha = \frac{x_2^{(2)} - x_2^{(1)}}{x_1^{(2)} - x_1^{(1)}}.$$

The group velocity $g^{\text{hom},(1)}$ in equation (25) is computed using the already found components of the slowness vector $\mathbf{p}^{\text{hom},(1)}$ and their derivatives obtained from equation (18),

$$g^{\text{hom},(1)} = \sqrt{\sum_{i=1}^3 \left(g_i^{\text{hom},(1)} \right)^2} = \frac{\sqrt{1 + \left(q_1^{\text{hom},(1)} \right)^2 + \left(q_2^{\text{hom},(1)} \right)^2}}{q^{\text{hom},(1)} - q_1^{\text{hom},(1)} p_1^{\text{hom},(1)} - q_2^{\text{hom},(1)} p_2^{\text{hom},(1)}}. \quad (26)$$

Equations (24) and (25) allow us to continue the traveltimes measured at level $z^{(0)}$ onto level $z^{(1)}$. The traveltime $t^{\text{LH},(2)}$ recorded at $[x_1^{(1)}, x_2^{(1)}, z^{(0)}]$ is mapped onto traveltime

$$t^{\text{LH},(2)} = t^{\text{LH}}(2) - t^{\text{LH},(1)} \quad (27)$$

at $[x_1^{(2)}, x_2^{(2)}, z^{(1)}]$. Then, using the measured vertical slowness $q^{\text{LH},(2)}$, we perform the parameter estimation step for the second interval between the depths $z^{(1)}$ and $z^{(2)}$, and find the vector $\chi^{(2)} = [V_0^{(2)}, \epsilon^{(2)}, \delta^{(2)}, \nu^{(2)}, \beta^{(2)}]$.

Although the entire process can be repeated as many times as desirable, it may lead to increasing errors in estimated parameters as we go from one interval to another. The main source of errors are inaccuracies in the derivatives $q_{,i}^{\text{hom},(n)} = \partial q^{\text{hom},(n)} / \partial p_i^{\text{hom},(n)}$ (n is the number of an interval), determining the directions of downward propagating rays in equation (24). The slowness components are the derivatives of measured traveltimes and, therefore, contain a higher level of errors than the traveltimes themselves. Taking

Layer	V_0	ϵ	δ	ν	β
Correct model parameters					
1	2.00	0.15	0.10	70.0	0.0
2	2.30	0.20	0.15	60.0	20.0
3	2.50	0.25	0.15	50.0	40.0
Inverted parameters					
LH is accounted for					
1	1.98	0.16	0.10	70.4	0.0
2	2.25	0.24	0.16	58.0	19.6
3	2.47	0.28	0.18	49.1	37.9
LH is ignored					
1	2.02	0.13	0.11	90.0	0.0
2	2.34	0.14	0.07	65.8	29.9
3	2.55	0.19	0.04	56.7	58.1

Table 5. Parameters of correct and inverted three-layered models. The layer thicknesses are 0.95, 0.40, and 0.10 km. Lateral velocity variations in the layers are linear: $f^{(1)} = 1 + 0.05x_1$, $f^{(2)} = 1 - 0.04x_1 - 0.02x_2$, and $f^{(3)} = 1 + 0.03x_2$. Velocity V_0 is given in km/s, the tilt ν and azimuth β of the symmetry axis – in degrees.

the derivative $\partial q^{\text{hom},(n)} / \partial p_i^{\text{hom},(n)}$, we differentiate the traveltimes twice, further amplifying those errors. The correction for LH is also a potential source of errors because it is the approximation designed for weak lateral heterogeneity. Correcting the data for LH in each interval, we introduce some errors. These errors are cascaded and may grow as we go deeper. Another inherent limitation of the technique is evident from equation (27): when the interval traveltime $t^{\text{LH},(n)}$ is small, its relative error is large. Therefore, parameters estimated for thinner intervals may be associated with greater errors. Overall, if the described procedure is applied to a large number of relatively thin intervals, the reliability of inverted anisotropic parameters may be questionable.

To illustrate the performance of correction for LH in layered media, we invert parameters of a three-layer LH TTI model. The correct model parameters are given in Table 5.

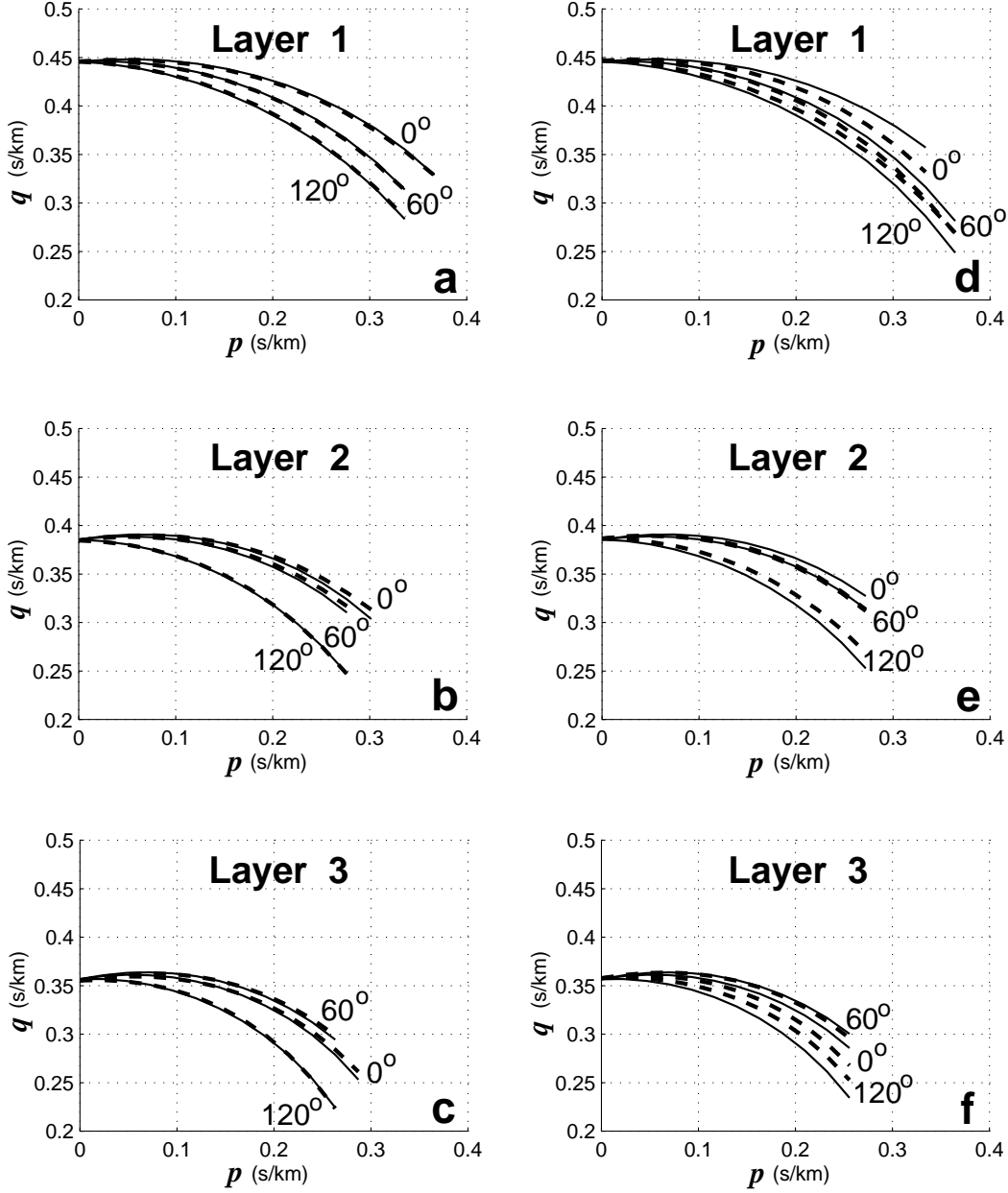


FIG. 9: Cross-sections of the correct slowness surfaces at azimuths $\alpha = 0^\circ$, 60° , and 120° (solid) in the three-layer LH VTI model given in Table 5 and the reconstructed cross-sections (dashed). Lateral heterogeneity has been estimated and removed in (a), (b), (c), and ignored in (d), (e), (f).

Figure 9a–9c shows the cross-sections of the slowness surfaces in the model layers after correcting for LH (dashed). There are some deviations of the reconstructed cross-sections from the correct ones (solid). These deviations lead to errors in inverted parameters of TTI layers (Table 5). The errors, however, are relatively small and do not exceed 0.04 for anisotropic coefficients ϵ and δ and 2.1° for the tilt ν of the symmetry axis and its azimuth β . For

comparison, we show the cross-sections obtained ignoring the influence of LH (Figure 9d – 9f). Clearly, the difference between the correct and reconstructed slowness surfaces became more significant. As a result, the inverted anisotropy parameters (Table 5) contain greater errors. The errors in the values of ϵ and δ reach 0.11, and in ν and $\beta - 20^\circ$. This example illustrates that, although the developed correction for LH does not produce perfect inversion results, the errors in estimated interval parameters are smaller than those obtained when LH is ignored.

VI. DISCUSSION

Lateral heterogeneity may introduce substantial errors in anisotropic parameters inverted from multi-azimuth walkaway VSP data. We have shown that the presence of LH can be identified from the VSP data and developed the procedure to remove its influence on estimated anisotropic parameters. Our technique is based on the relation $t = (\mathbf{p} \cdot \mathbf{x})$ between traveltime t in a homogeneous arbitrary anisotropic medium, the slowness vector \mathbf{p} , and the difference \mathbf{x} between coordinates of a source and a receiver. VSP geometry allows one to measure all quantities in this equation directly. Thus, we can explicitly check if the data satisfy the hypothesis of homogeneity. If they do not, there is a choice of attributing the deviation of t from $(\mathbf{p} \cdot \mathbf{x})$ to either vertical or lateral heterogeneity. We have shown that the same data may correspond to heterogeneity of either type. Therefore, it appeared that the only way to separate the two kinds of heterogeneity in VSP geometry is to estimate vertical inhomogeneity explicitly, using the data obtained at a sufficiently dense set of downhole receivers. We have developed a procedure to account for LH in vertically varying media.

The important assumption we have made is that anisotropy is factorized within each depth interval. The physical meaning of this assumption is that velocity heterogeneity makes greater contribution to recorded traveltimes than variations in anisotropic coefficients. Based on that, we ignored these variations. The assumption of factorized anisotropy allowed us to separate the influences of lateral heterogeneity and anisotropy on the data. In fact, we effectively reduced the number of parameters which determine the traveltimes in VSP geometry and, thus, removed the otherwise existing null-space of our inverse problem. Note that, after LH has been accounted for, all five parameters specifying P -wave kinematics in transversely isotropic media with a tilted axis of symmetry – $V_0, \epsilon, \delta, \nu, \beta$ – can be

unambiguously estimated. In this regard, VSP data are different from the P -wave reflection traveltimes that constrain these five parameters independently only when the tilt ν exceeds $30^\circ - 40^\circ$ [6].

We have also assumed that LH is weak. Although this assumption was not necessary from the standpoint of parameter estimation, it allowed us to obtain explicit equations describing the influence of lateral heterogeneity. We showed that these equations can be inverted and the lateral velocity variation can be found from traveltimes recorded in a VSP geometry. The approximate nature of the derived expressions does introduce some errors in estimated anisotropic parameters; however, our numerical examples have demonstrated that those errors are small compared to the errors produced by applying the conventional methodology that simply ignores the presence of lateral heterogeneity.

Acknowledgments

We are grateful to members of the A(nisotropy)-Team of the Center for Wave Phenomena (CWP) at CSM for helpful discussions. P. Contreras thanks PDVSA-INTEVEP for supporting his visit to the CWP. The support for this work was provided by the members of the Consortium Project on Seismic Inverse Methods for Complex Structures at CWP and by the United States Department of Energy (award #DE-FG03-98ER14908).

-
- [1] Alkhalifah, T., and Tsvankin, I., 1995, *Geophysics*, **60**, 1550–1566.
 - [2] Backus, G. and Gilbert, F., *Bull. Seism. Soc. Am.* **59** (1969) 1407.
 - [3] Gaiser, J., *J. Geophys. Res.*, **95**, (1990) 11241.
 - [4] Grechka, V. and McMechan, G., *Geophysics* (1996) **61**, 1883
 - [5] Grechka, V. and Tsvankin, I., 67th Ann. Internat. Mtg., Soc. Expl. Geophys., Expanded Abstracts, (1997) 1226.
 - [6] Grechka, V. and Tsvankin, I., 68th Ann. Internat. Mtg., Soc. Expl. Geophys., Expanded Abstracts, (1998) 1483.
 - [7] Contreras P., Klie H., and Michelena R., 68th Ann. Internat. Mtg. Soc. Expl. Geophys. (1998) 1491.

- [8] Miller, D.E., and Spencer, C., 1994, *J. Geophys. Res.*, **99**, 21651–21657.
- [9] Miller, D., Leaney, S., and Borland, W., *J. Geophys. Res.*, **99** (1994) 21659.
- [10] Musgrave, M. *Crystal Acoustics*. Holden-Day (1970).
- [11] Grechka, V. and Mateeva, A. *Geophysics*. **72(4)** (2007) D69-D79.
- [12] Press, W., Flannery, B., Teukolsky, S. and Vetterling, W., *Numerical recipes: the art of scientific computing*. Cambridge University Press (1987)
- [13] P. Contreras, G. Larrazabal and C. Florio **arXiv** 1901.00255v1 (2018).
- [14] Sayers C., *Geophysics*. **62** (1997) 723.
- [15] Thomsen L., *Geophysics*. **51** (1986) 1954.